Available online at www.sciencedirect.com

Dyes and Pigments 63 (2004) 161–168

www.elsevier.com/locate/dyepig

Investigations on the solubilities of some disperse azo dyes in supercritical carbon dioxide

Javad Fasihi[a], Yadollah Yamini[a,*], Farahnaz Nourmohammadian[b], Naader Bahramifar[a]

[a]*Department of Chemistry, Tarbiat Modarres University, P.O. Box 14115-175, Tehran, Iran*
[b]*Department of Manufacture of Colorant, Iran Color Research Center, Tehran, Iran*

Received 26 October 2003; received in revised form 12 December 2003; accepted 27 January 2004

Abstract

The solubilities of three disperse azo dyes, 4-(*N*,*N*-dimethylamino)-4′-nitroazobenzene (D_1), 4-(*N*,*N*-diethylamino)-4′-nitroazobenzene (D_2) and Parared (D_3) in supercritical carbon dioxide have been measured at different temperatures (308, 318, 328, 338, 348 and 358 K) and in the pressure range of 122–355 bar. The measurements were performed using a simple static method. As evidenced from the experimental results, the solubilities increase with increasing density of supercritical CO_2. The solubilities in supercritical CO_2 decrease in the order $D_2 > D_1 > D_3$, which parallel the order of their relative melting points; the higher the melting point, the lower the solubility. The equilibrium solubility data were correlated using a semiempirical model. The calculated results show satisfactory agreement with the experimental data.

Keywords: Solubility; Disperse azo dyes; Supercritical carbon dioxide

1. Introduction

In light of environmental concern, the textile industry has accelerated efforts to reduce or eliminate water consumption in all areas of yarn preparation, dyeing, and finishing. Supercritical fluid dyeing technology has the potential to accomplish this objective in many commercial textile applications around the world [1–4]. Based on statements of German federal statistics concerning water consumption of (West) German industry during 1987, the textile producing branches consumed about 282.4 million m^3 of water, of which a main part is required in processing steps. Even if those data describe a situation that existed some years ago, a severe demand for reducing water consumption and thus reducing wastewater pollution still exists notwithstanding the aspect of costs [5].

Supercritical carbon dioxide (SC-CO_2) is one of the most environmentally acceptable solvents in use today, and textile processes using this solvent have many advantages when compared to conventional aqueous processes. Supercritical fluids have very low surface tension, low viscosity, and high diffusivity, which enable easy penetration into the network of the textile and result in rather

---

[*] Corresponding author. Tel.: +98-21-800-6631; fax: +98-21-800-6544.

0143-7208/$ - see front matter © 2004 Elsevier Ltd. All rights reserved.
doi:10.1016/j.dyepig.2004.01.007

short dyeing times. In the process of supercritical dyeing, without using water and other liquid solvents, the following time consuming drying step is not required. The dissolved dyestuff can easily be separated from the supercritical fluid by simple expansion, thus both carbon dioxide and excess dye can be reused. Additional advantages would be elimination of expensive additives such as dispersing agents and surfactants used in conventional dyeing. Finally, this new cleaner dyeing technology appears to be economically attractive for the textile industry. However, it should be noted that only those disperse dyes or other nonionic compounds which are able to penetrate into the lipophilic polymeric materials, when dissolved in SC-CO_2, can be used in these treatments [6]. Since most dyes were developed specifically for water-based applications, they have been designed as water-soluble dyes, with very limited solubility in supercritical carbon dioxide. Hence, later studies were concentrated on identifying supercritical carbon dioxide soluble dyes.

SC-CO_2 solubility is one of the most important parameters for the dye selection and for the optimization of process temperature and pressure. Thus, solubility data are needed for the development of the supercritical dyeing processes. In this work, the solubilities of three disperse dyes, 4-(*N*,*N*-dimethylamino)-4′-nitroazobenzene (D_1), 4-(*N*,*N*-diethylamino)-4′-nitroazobenzene (D_2) and Parared (D_3) (Table 1) have been measured in supercritical carbon dioxide to assist with the design of the dyeing processes.

2. Experimental section

2.1. Apparatus and operation

All solubility measurements were performed using a Suprex (Pittsburgh, PA) MPS/225 system equipped with a modified static system in SFE mode. A detailed description of the construction and calibration of this method has been previously reported [7,8]. Briefly, a 1-ml high-pressure saturation cell was filled with a 10 mass% mixture of compound with clean glass beads to prevent channeling. The saturation cell was placed in the oven of the system to provide precise temperature control (±0.2 K) during the solubility determination. After thermal equilibrium in the oven was reached, a syringe pump was used in the constant pressure mode to supply pressurized CO_2 into the saturation cell. After equilibrium at desired temperature and pressure was reached (25 min), a 182 μl portion of the saturated supercritical CO_2 was loaded into the injection loop. It should be noted that by monitoring solubility data versus time, 25 min was

Table 1
Structure of dyes and their physicochemical properties

Dyes	Structure	Melting point (K)	λ_{max} (nm)	Mw (g mol^{-1})	Solvent
D_1	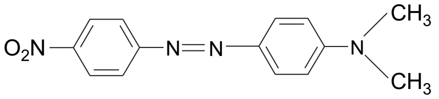	488–489	471	270.12	MeOH
D_2	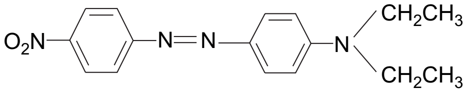	418–419	472	298.14	EtOH
D_3	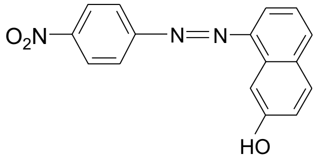	529–530	482	293.13	CH_3CN

found to be adequate to ensure the attainment of equilibrium. The loop was then depressurized into the collection vial containing a proper organic solvent (Table 1). Finally, the sample loop was washed with the same solvent and was collected in the collection vial. The final volume of the solution was 5 ml. Solubility determinations were performed at temperatures 308 K to 358 K and pressures from 122 bar to 355 bar. During a typical experiment, the oven temperature was held constant while the pressure was raised in 30 bar increments. The experimental uncertainty in this study is simulated to be ±0.5 bar for pressure. The solubilities were determined by absorbance measurements at suitable wavelength (λ) for each compound (Table 1) using a model 2100 Shimadzu UV–Vis spectrophotometer. The stock solutions of the solid samples were prepared by dissolving appropriate amounts of the solid samples in a proper solvent (Table 1). A set of five standard solutions was then prepared in the concentration range of 0.5–7 $\mu g\ ml^{-1}$. The calibration curves obtained (with regression coefficients better than 0.999) were used to establish the concentration of the dyes in the collection vial. The mole fraction compositions of the solutes were generally reproducible within ±3%.

2.2. Materials

Carbon dioxide (99.99%) was purchased from Sabalan Co. (Tehran, Iran). HPLC grade methanol, ethanol and acetonitrile (Merck) were used as received. The disperse azo dyes were obtained from the Iran Color Research Center (Tehran, Iran). The purities of disperse azo dyes were higher than 99 mass% and no further purification was done before use. However, prior to the measurement of solubilities, the dyes were extracted by dynamic SFE at $P = 152$ bar and $T = 308$ K for a duration of 10 min at the supercritical flow rate of 0.3 ml min^{-1}. After making sure that no impurities existed in the extract, solubility measurements were done. Some basic information for these disperse azo dyes is given in Table 1, in which T_m is the melting point that was measured by a melting point measurement instrument from GallenKamp Company (U.K.).

3. Results and discussion

The reliability and efficiency of the solubility measurement technique were previously established by measuring the solubility of naphthalene in supercritical CO_2 at 308 K and different pressures, as was described before [9,10]. The measured solubilities of naphthalene agreed within approximately 0.8% to 6.8% with those of previous measurements.

Solubility measurements of disperse dyes with static apparatus have shown that the spectrophotometric determination of concentrations is affected by even small concentrations of more soluble impurities absorbing in the same range of the spectrum as the dyestuff itself [11,12]. The flow method often allows an easy extraction of such impurities; the continuous purification can be observed as a characteristic change in the shape of the spectrum. Thus in the present work, small quantities of volatile impurities present were extracted by dynamic SFE, prior to the measurement of solubilities.

The solubility measurements were carried out at temperatures 308, 318, 328, 338, 348 and 358 K over a pressure range from 122 to 355 bar. The experimental results are listed in Table 2 in terms of equilibrium mole fraction, y, and in grams per liter, s, of the solute. The reported values are the average of at least three replicate measurements with percentage relative standard deviations less than ±5%.

The densities of CO_2 calculated by the Suprex "SF-Solver" at various pressures and temperatures used for the dye solubility determinations are also included in Table 2. The Suprex "SF-Solver" uses the modified equation of state extended to include high-pressure fluids as proposed by Pitzer [13] and Pitzer et al. [14].

The data given in Table 2 reveal that the solubility of D_2 is greater than that of D_1 and D_3 by a factor of about 7 and 20, respectively. The addition of one CH_2-group to D_2 molecule, results in a significant solubility enhancement of D_2 in comparison with D_1. Similar results have been reported in the literature [15]. The ability to form either inter- or intra-molecular hydrogen bonds promotes mutual solute interactions and consequently, the solubilization in CO_2 is hindered [15].

Table 2
Solubilities of three disperse azo dyes, D_1, D_2, and D_3 in SF-CO_2 at various temperatures and pressures

Parameters			D_1		D_2		Parameters			D_3	
T (K)	P (bar)	ρ (kg m^{-3})	s (g L^{-1})	$10^6\ y$	s (g L^{-1})	$10^5\ y$	T (K)	P (bar)	ρ (kg m^{-3})	$10^2\ s$ (g L^{-1})	$10^6\ y$
308	122	771	0.014	2.93	0.049	0.93	328	122	516	0.11	0.32
	152	818	0.014	2.74	0.620	1.12		152	657	0.21	0.48
	182	850	0.014	2.61	0.870	1.51		182	726	0.38	0.78
	213	876	0.016	2.93	0.100	1.76		213	771	0.6	1.16
	243	897	0.020	3.61	0.130	2.11		243	804	0.77	1.45
	274	916	0.022	3.83	0.150	2.36		274	831	0.96	1.73
	304	931	0.022	3.81	0.160	2.6		304	853	1.17	2.06
	334	946	0.027	4.62	0.190	2.91		334	872	1.43	2.46
	355	955	0.028	4.84	0.200	3.16		355	884	1.62	2.75
318	122	661	0.006	1.46	0.036	0.8	338	122	396	0.12	0.44
	152	745	0.010	2.12	0.063	1.25		152	561	0.19	0.50
	182	792	0.014	2.83	0.089	1.66		182	654	0.33	0.75
	213	826	0.018	3.50	0.110	1.97		213	712	0.68	1.43
	243	852	0.022	4.21	0.160	2.73		243	754	0.89	1.77
	274	875	0.023	4.20	0.170	2.88		274	786	1.27	2.43
	304	893	0.026	4.74	0.180	2.93		304	812	1.67	3.08
	334	910	0.028	5.07	0.250	4.09		334	834	1.95	3.51
	355	919	0.035	6.23	0.270	4.36		355	848	2.23	3.95
328	122	516	0.006	2.00	0.018	0.51	348	122	327	0.13	–
	152	657	0.010	2.05	0.038	0.85		152	477	0.13	0.41
	182	726	0.013	2.89	0.070	1.41		182	585	0.41	1.06
	213	771	0.020	4.23	0.120	2.22		213	652	0.54	1.25
	243	804	0.023	4.61	0.160	2.93		243	702	0.91	1.95
	274	831	0.027	5.37	0.180	3.26		274	740	1.43	2.90
	304	853	0.037	7.06	0.250	4.33		304	772	1.80	3.50
	334	872	0.044	8.27	0.300	5.12		334	796	2.31	4.35
	355	884	0.060	9.85	0.330	5.6		355	811	2.79	5.16
338	122	396	0.004	1.65	0.008	0.28	358	122	287	0.04	0.22
	152	561	0.090	2.08	0.030	0.79		152	406	0.13	0.47
	182	654	0.014	3.37	0.066	1.48		182	517	0.27	1.27
	213	712	0.022	4.94	0.027	2.36		213	593	0.54	2.22
	243	754	0.030	6.57	0.200	3.9		243	650	1.18	2.85
	274	786	0.039	8.05	0.250	4.77		274	693	1.75	3.80
	304	812	0.051	10.30	0.340	6.23		304	728	2.31	4.76
	334	834	0.061	11.99	0.420	7.46		334	757	2.98	5.91
	355	848	0.072	13.77	0.490	8.55		355	774	3.33	6.46
348	122	327	0.003	1.59	0.005	0.24					
	152	477	0.007	2.03	0.025	0.76					
	182	585	0.014	3.71	0.060	1.52					
	213	652	0.025	6.22	0.130	2.88					
	243	702	0.035	8.01	0.270	5.75					
	274	740	0.044	9.78	0.350	7.07					
	304	772	0.060	12.62	0.430	8.28					
	334	796	0.066	15.22	0.530	9.92					
	355	811	0.091	18.37	0.610	11.1					

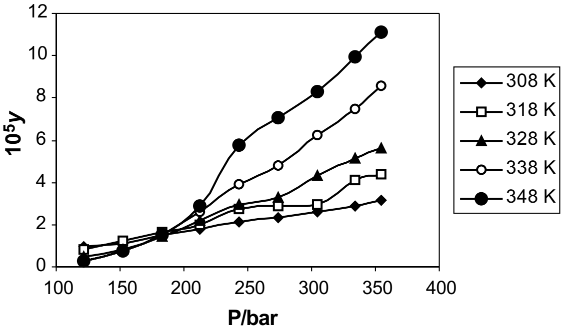

Fig. 1. Equilibrium mole fraction of D_2 as a function of pressure.

We presume that the intermolecular hydrogen bonds are responsible for poor solubility of D_3 in SF-CO_2. Moreover, the solubilities parallel the order of the relative melting points; the higher the melting point, the lower the solubility. Also it is observed that, in general, the solubility increases by increasing the pressure of CO_2. This may be due to the increased density of CO_2 with increasing pressure, since the CO_2 density is directly related to its dissolving power [16]. By examining the effect of temperature on the solubilities, we can find out the existence of a retrograde (crossover pressure effect) behavior for all three dye molecules at about 180 bar, as was reported for different organic compounds previously [7–9]. It is worth pointing out that the crossover point is difficult to see from Table 1, but it can be easily observed from the mole fractions versus pressure isotherms (Fig. 1). Two competing effects can explain this effect. In principal, increasing temperature favors solubility via increase in vapor pressure of the dye, but at the same time the solvent density decreases. At low pressures the decrease of solvent density dominates, and the overall solubility of the dye decreases with increasing temperature. At higher pressures the solubilities increase with rising temperatures, because the densities in this range only slightly depend on temperature, and the normal temperature dependence of solubility dominates [17]. This

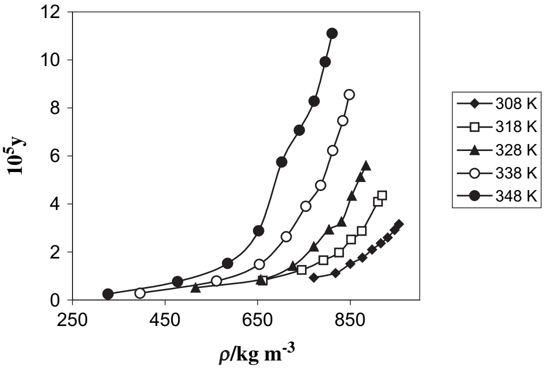

Fig. 2. Equilibrium mole fraction of D_2 as a function of pure carbon dioxide density.

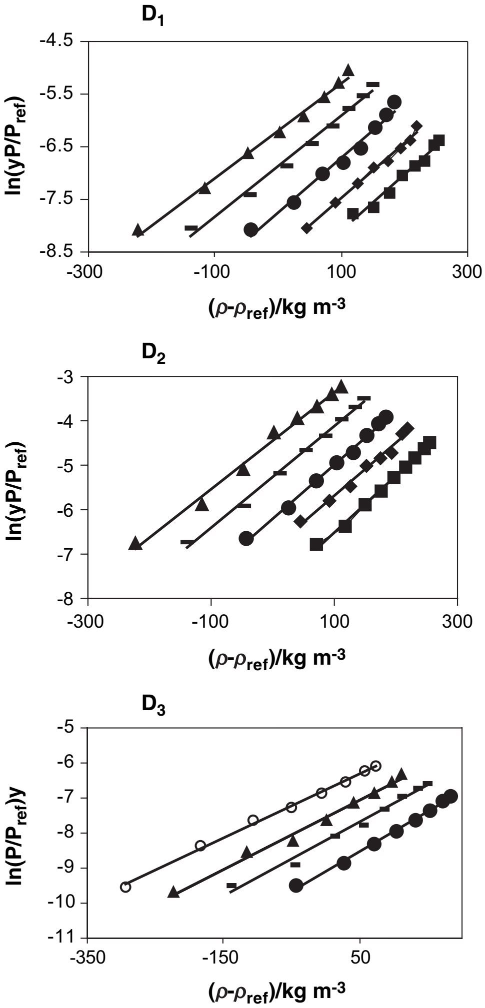

Fig. 3. Plots of isotherms of $\ln(yP/P_{ref})$ versus density for three azo dyes at temperatures 308 (■), 318 (♦), 328 (●), 338 (▬), 348 (▲) and 358 K (○).

Table 3
Solubility constants a, b, and C and the estimated ΔH_{vap} values and AARD% obtained from the data correlation procedure

Dye	a	b (K)	C ($\mathrm{kg^{-1}\ m^3}$)	ΔH_{vap} ($\mathrm{kJ\ mol^{-1}}$)	AARD%[a]
D_1	16.23	−7820.1	0.010	65	6.36–17.68
D_2	19.86	−8489.3	0.012	71	5.97–16.03
D_3	14.15	−7529.7	0.0082	63	13.05–25.45

[a] $\mathrm{AARD\%} = 100/N \times \{\sum (y^{\mathrm{exp}} - y^{\mathrm{cal}})/y^{\mathrm{cal}}\}$ where y^{exp} and y^{cal} are the experimental and calculated solubility values, respectively; and N is the number of data points.

explanation is supported by the concentration versus density plot where intersection points are no longer found (Fig. 2).

3.1. Correlation of the solubility data

The dye solubilities in SC-CO_2 are difficult to predict and the solubility data, if not completely determined experimentally, must be obtained by fitting equations to existing experimental data. In this work, the correlations were based on the concept of solubility enhancement [18] from which the following equations were derived from [19]:

$$\ln(yP/P_{\mathrm{ref}}) = A + C(\rho - \rho_{\mathrm{ref}}) \tag{1}$$

where y is the mole fraction of solute (taken here to be equal to the ratio of the number of moles of solute divided by the number of moles of carbon dioxide), P is the pressure, P_{ref} is a standard pressure of 1 bar, ρ is the density of solution (taken as the density of pure carbon dioxide), ρ_{ref} is a reference density with a value of 700 $\mathrm{kg\ m^{-3}}$, and A and C are constants. ρ_{ref} is used so that the intercept A is within the experimental data range and does not suffer the variability experienced, if an intercept extrapolated to zero density is used [20]. The constant C, resulting physically from solvation by the fluid, is assumed to be constant over the temperature range and constant A, arising from the vapor pressure (fugacity) of the solute, is given by:

$$A = a + b/T \tag{2}$$

where a and b are constants and T is the absolute temperature. When Eqs. (1) and (2) are combined, the overall correlation equation is obtained to be:

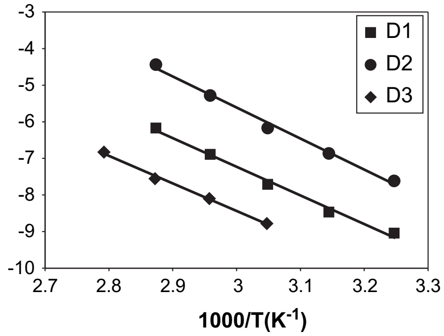

Fig. 4. Plot of A as a function of $(1/T)$ for three disperse dyes.

$$\ln(yP/P_{\mathrm{ref}}) = a + b/T + C(\rho - \rho_{\mathrm{ref}}) \tag{3}$$

In the first step, $\ln(yP/P_{\mathrm{ref}})$ values were plotted against density (Fig. 3), and the values were fitted to a straight line by the least squares regression to estimate the C and A parameters. According to Eq. (1), the resulting plots are expected to be straight lines of similar slopes (correlation coefficients, r^2, of the lines are better than 0.99). The values of C, obtained from the slopes of the corresponding plots, were then averaged for each compound (Table 3).

The plots of A versus $1/T$ for each compound resulted in straight lines (Fig. 4), from the intercept and slope of which the a and b values were obtained, respectively. The resulting a and b values for compounds are also included in Table 3. Finally, the values of a, b, and C were used to predict solubility from Eq. (3). Fig. 5 compares the calculated isotherms with the experimental data. As is obvious, the Bartle method provided a good fit, with absolute average relative deviations (AARD) in the range of 6% to 25% for D_1 to D_3 at different temperatures (Table 3).

The parameter b is approximately related to the enthalpy of vaporization of the solid, ΔH_{vap}, by:

$$\Delta H_{\mathrm{vap}} = -Rb \tag{4}$$

where R is gas constant. A detailed physical description of this relation was given by Miller

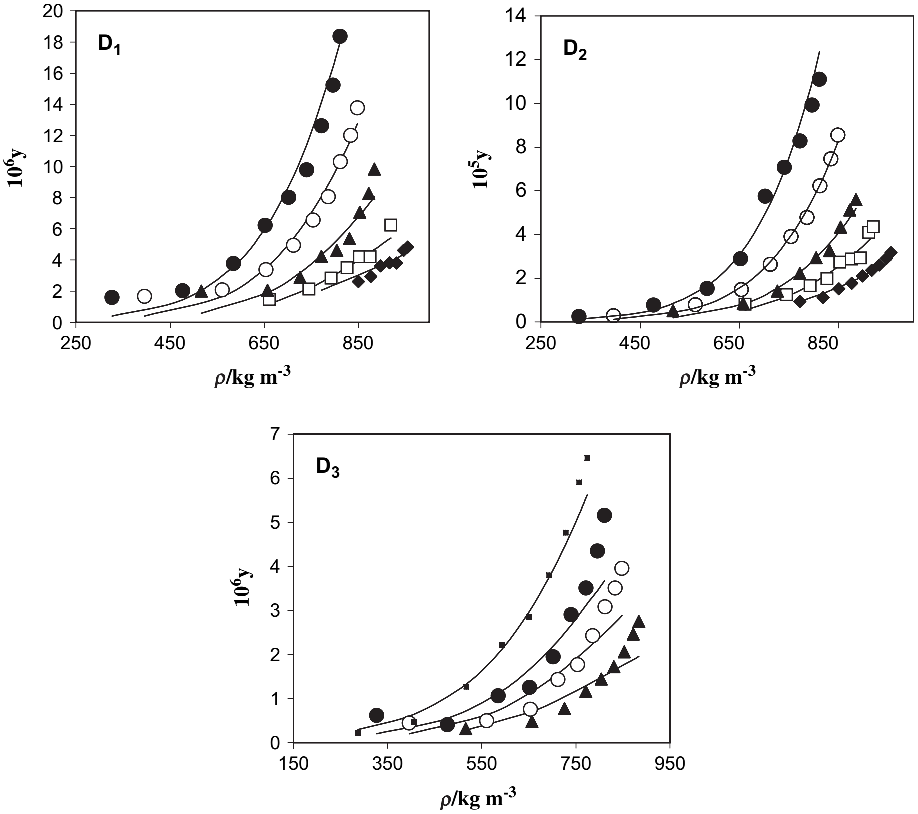

Fig. 5. Comparison of experimental (point) and calculated (line) solubilities at temperatures, 308 (◆), 318 (□), 328 (▲), 338 (○), 348 (●), 358 (■) for D_1 to D_3.

et al. [20]. The resulting ΔH_{vap} values are also presented in Table 3.

References

[1] Park MW, Bae HK. Dye distribution in supercritical dyeing with carbon dioxide. J Supercrit Fluids 2002;22:65–73.

[2] Rita De Giorgi M, Candoni E, Maricca D, Piras A. Dyeing polyester fibers with disperse dyes in supercritical CO_2. Dyes Pigments 2000;45:75–9.

[3] Sicardi S, Manna L, Banchero M. Diffusion of disperse dyes in PET films during impregnation with a supercritical fluid. J Supercrit Fluids 2000;17:187–94.

[4] Lin HM, Liu CY, Cheng CH, Chen YT, Lee MJ. Solubilities of disperse dyes of blue 79, red 153, and yellow 119 in supercritical carbon dioxide. J Supercrit Fluids 2001;21:1–9.

[5] Knittel D, Schollmeyer E. Prevention of water pollution in dyeing processes of synthetic textiles. Eur Water Pollut Control 1996;6:6–9.

[6] Beltrame PL, Castelli A, Selli E, Mossa A, Testa G, Bonfatti AM, et al. Dyeing of cotton in supercritical carbon dioxide. Dyes Pigments 1998;39:335–40.

[7] Yamini Y, Bahramifar N. Solubilities of polycyclic aromatic hydrocarbons in supercritical carbon dioxide. J Chem Eng Data 2000;45:53–6.

[8] Fat'hi MR, Yamini Y, Sharghi H, Shamsipur M. Solubilities of some recently synthesized 1,8-dihydroxy-9,10-anthraquinone derivatives in supercritical carbon dioxide. Talanta 1999;48:951–7.

[9] Fat'hi MR, Yamini Y, Sharghi H, Shamsipur M. Solubilities of some 1,4-dihydroxy-9,10-anthraquinone derivatives in supercritical carbon dioxide. J Chem Eng Data 1998;43:400–2.

[10] Yamini Y, Fat'hi MR, Alizadeh N, Shamsipur M. Solubilities of dihydroxy benzene isomers in supercritical carbon dioxide. Fluid Phase Equilib 1998;152:299–305.

[11] Haarhaus U, Swidersky P, Schneider GM. High-pressure investigation on the solubility of disperse dyestuffs in

supercritical gases by VIS/NIR spectroscopy. Part I. J Supercrit Fluids 1995;8:100–6.
[12] Swidersky P, Tuma GM, Schneider GM. High-pressure investigation on the solubility of anthraquinone dyestuffs in supercritical gases by VIS/NIR spectroscopy. Part II. J Supercrit Fluids 1996;9:12–8.
[13] Pitzer KS. The volumetric and thermodynamic properties of fluids. I. Theoretical basis and virial coefficients. J Am Chem Soc 1995;77:3427–33.
[14] Pitzer KS, Lippman DZ, Curl Jr RF, Huggins CM, Petersen DE. The volumetric and thermodynamic properties of fluids. II. Compressibility factor, vapor pressure and entropy of vaporization. J Am Chem Soc 1955;77:3433–40.
[15] Draper SL, Montero GA, Smith B, Beck K. Solubility relations for disperse dyes in supercritical carbon dioxide. Dyes Pigments 2000;45:177–83.
[16] Koga Y, Iwai Y, Arai Y. Monte-Carlo simulation for chain molecules in supercritical ethane. J Chem Phys 1994;101:2283–8.
[17] Wagner B, Kautz CB, Schneider GM. Investigations on the solubility of anthraquinone dyes in supercritical carbon dioxide by a flow method. Fluid Phase Equilib 1999;158–160:707–12.
[18] Johnston K, Peck DG, Kim S. Modeling supercritical mixtures: how predictive is it? Ind Eng Chem Res 1989;28:1115–25.
[19] Bartel KD, Clifford AA, Jafar SA, Shilstone GF. Solubilities of solids and liquids of low volatility in supercritical carbon dioxide. J Phys Chem Ref Data 1991;20:713–56.
[20] Miller DJ, Hawthorne SB, Clifford AA, Zhu S. Solubility of polycyclic aromatic hydrocarbons in supercritical carbon dioxide. J Chem Eng Data 1996;41:779–86.